Available online at www.sciencedirect.com
SCIENCE DIRECT®
International Journal of Heat and Mass Transfer 48 (2005) 4062–4072
International Journal of HEAT and MASS TRANSFER
www.elsevier.com/locate/ijhmt

Momentum and heat transfer in a turbulent cylinder wake behind a streamwise oscillating cylinder

G. Xu, Y. Zhou *

Department of Mechanical Engineering, The Hong Kong Polytechnic University, Hung Hom, Kowloon, Hong Kong

Received 22 March 2004; received in revised form 16 March 2005

Abstract

The work aims to understand the effect of an oscillating circular cylinder on momentum and heat transport in the turbulent wake of a downstream identical cylinder, which is slightly heated. The oscillating amplitude, A, was $0.79d$ (d is the cylinder diameter) and the frequency was $0.17f_s$ for $L/d = 2.5$ and $0.24f_s$ for $L/d = 4$, where L and f_s are the cylinder centre-to-centre spacing and the frequency of vortex shedding from the downstream cylinder, respectively, at $A = 0$. The velocity and temperature fields were measured using a three-wire probe at $10d$ behind the stationary cylinder and a Reynolds number of 5920 based on d and the free-stream velocity. It is found that the upstream cylinder oscillation modifies the frequency of vortex shedding from the stationary cylinder, which is locked on with one harmonic of the oscillating frequency. This harmonic frequency is nearest to and below the natural vortex-shedding frequency. Furthermore, the wake response to the oscillation depends on L/d in terms of the cross-stream distributions of mean velocity, Reynolds stresses, temperature variance and heat fluxes; the turbulent Prandtl number decreases at $L/d = 4$ but increases at $L/d = 2.5$. The observations are linked to whether the flow regime experiences a change under the upstream cylinder oscillation.

Keywords: Turbulent wake; Two tandem cylinder wake; Momentum and heat transfer; Streamwise oscillating cylinder

1. Introduction

The turbulent flow behind multiple slender cylinders has received significant attention in the past [1–3]. It is of both fundamental and practical significance to understand the momentum and heat transfer characteristics of this flow. The simplest configuration of multiple cylinders is two in tandem, side-by-side and staggered arrangements. Aerodynamic interference between two cylinders involves most of the generic flow features associated with multiple structures; the study of this flow may provide insight into flow physics and heat transport around more cylinders [4–7].

Using a laser-Doppler velocimeter, Kolář et al. [4] conducted ensemble-averaged measurements in the turbulent near wake of two side-by-side square cylinders at $T^* = 3$ and $Re = 23\,100$, where, T is transverse spacing between the two cylinder axes, d is the characteristic height of the cylinder, Re is Reynolds number based on d and free-stream velocity U_∞. Unless otherwise stated, an asterisk in this paper denotes normalization by either U_∞, d or temperature excess Θ_0. They found that the inner vortices close to the flow centreline decayed

* Corresponding author. Tel.: +852 2766 6662.
E-mail address: mmyzhou@polyu.edu.hk (Y. Zhou).

0017-9310/$ - see front matter © 2005 Elsevier Ltd. All rights reserved.
doi:10.1016/j.ijheatmasstransfer.2005.04.029

more rapidly than the outer ones shed from the cylinder side near the free stream. Based on flow visualization and particle image velocimetry (PIV) measurements, Sumner et al. [5] investigated the flow around two circular cylinders of the same diameter in a staggered arrangement with a centre-to-centre pitch ratio $P^* = 1$–5 and an angle of incidence $\alpha = 0$–90° for $Re = 850$–1900, and identified nine flow patterns depending on P and α. Using a phase-averaging method [8], Zhou et al. [7] studied the momentum and heat transport in the wake of two side-by-side circular cylinders at $Re = 5800$ and found that the flow structure at $T^* = 3$ was totally different from that at $T^* = 1.5$, the two flow regimes showing distinct momentum and heat transport characteristics.

The flow around two tandem cylinders has also attracted considerable attention. This flow may be classified into three regimes [1,2]. For $1 < L^* < 1.2$–1.8, where L is the cylinder centre-to-centre spacing, free shear layers separating from the upstream cylinder overshoot the downstream one and then roll up into vortices. For 1.2–$1.8 < L^* < 3.4$–3.8, the shear layers reattach on the upstream side of the downstream cylinder. A vortex street is formed only behind the latter. For $L^* > 3.4$–3.8, both cylinders generate vortices. Yiu et al. [9] measured flow and temperature fields behind two stationary tandem cylinders with the downstream one slightly heated. Their measurements covered the three regimes, i.e., $L^* = 1.3$, 2.5 and 4.0. They found that vortical structures, momentum and heat transport were strongly dependent on the flow regimes.

The initial conditions may have a profound effect on a flow. The effects of initial conditions on turbulent wakes may persist far downstream [10]. The equilibrium similarity analysis [11] indicated that the initial conditions and local Reynolds number effects dominated an axisymmetric wake, and this dependence on upstream conditions was asymptotic. Zhou and Antonia [12] examined the memory effects in turbulent plane wakes generated by circular, triangular and square cylinders and a screen of 50% solidity, respectively. Discernible differences in Reynolds stresses, fluctuating velocity spectra and root mean square vorticities were observed for different generators even in the far wake. In engineering, the structures such as offshore pilings and heat exchangers are frequently associated with flow-induced oscillation. The structural oscillation alters the initial conditions and may affect the momentum and heat transport of the flow. In an experimental study of the flow structure and heat transfer over a heated cylinder oscillating at a small amplitude in the stream direction, Gau et al. [13] demonstrated that an oscillation frequency near twice the natural vortex-shedding frequency enhanced heat transfer. Lai et al. [14] found that an oscillating cylinder could even lock in vortex shedding from a neighbouring side-by-side arranged cylinder. Mahir and Rockwell [15,16] investigated vortex formation around two forced oscillating cylinders in the tandem and side-by-side arrangements. However, there is a lack of information on how the cylinder oscillation would alter the momentum and heat transport in the turbulent wake of two inline cylinders.

This work aims to understand how an upstream oscillating cylinder influences the flow and temperature fields in a turbulent cylinder wake. Two L^* values, i.e. 2.5 and 4, are investigated, covering two of the three flow regimes in the absence of cylinder oscillation [2]. The flow regime of very small L^* is not investigated due to a difficulty in carrying out oscillating-cylinder experiments at small L^*. The investigation is conducted at a fixed oscillation amplitude $A^* = 0.79$ and frequency $f_e^* = 0.025$, resulting in a frequency ratio $f_e/f_s = 0.17$ at $L^* = 2.5$ and 0.24 at $L^* = 4$, where the frequency f_s of vortex shedding from two stationary cylinders depends on L^* [1,17]. A relatively low f_e/f_s is selected in view of the fact that past investigations are frequently conducted on the condition of synchronization, i.e. $f_e \approx f_s$, and the data of a small f_e/f_s are scarce. More experimental details are given in Section 2. The results are presented in Sections 3–5 and concluded in Section 6.

2. Experimental conditions

Experiments were carried out in a close-circuit wind tunnel with a 2.4 m long square working section of 0.6 m × 0.6 m. The details of the tunnel were given in [7]. The wake was generated by two circular cylinders of the same diameter $d = 0.0127$ m, arranged in tandem (Fig. 1). The cylinders had an aspect ratio of 17 and were cantilever-supported in the horizontal mid-plane of the working section, causing a blockage of 2.1%. In order to reduce the end effects, circular plates with a diameter of 0.12 m and a thickness of 0.002 m, designed following Stansby's recommendations [18], were mounted at both ends of the cylinders. The longitudinal spacing between the cylinders, L^*, is 2.5 and 4, respectively. The upstream cylinder, made of aluminium, was forced to oscillate

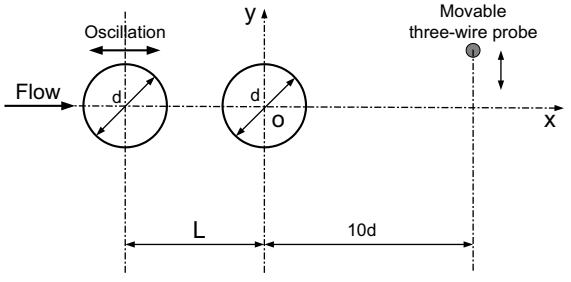

Fig. 1. Schematic arrangement of measurements.

longitudinally by a computer-controlled motor system, which allowed the accurate adjustment of the oscillation frequency and amplitude. The downstream cylinder, made of brass, was slightly heated electrically. The maximum mean temperature of the heated wake was about 0.8 °C above ambient, implying a negligible buoyancy effect and heat may be considered to be a passive scalar. Unless otherwise stated, all temperatures in the paper are given with respect to ambient.

Experiments were conducted at $Re = 5920$ and $x^* = 10$ with and without the upstream cylinder oscillating ($A^* = 0.79$). The coordinates x and y are defined in Fig. 1. The oscillation frequency was fixed at $f_e^* = 0.025$, resulting in a frequency ratio of $f_e/f_s = 0.17$ for $L^* = 2.5$ and 0.24 for $L^* = 4$ since f_s is dependent on L^* [1,17]. The choice of such a low f_e/f_s ratio allows the oscillation effect to be investigated in the absence of vortex shedding 'locked-on' with f_e.

A three-wire probe consisting of an X-wire and a cold wire was used to measure the longitudinal velocity (u), transverse velocity (v) and temperature (θ) fluctuations. The cold wire was placed orthogonally to the plane of the X-wire and about 0.8 mm upstream of the X-wire intersection. The probe was mounted on a traversing mechanism controlled by a personal computer, which allowed motion in three directions, with a resolution of 0.1 mm and 0.01 mm in the streamwise and cross-stream directions, respectively. The sensing elements of the X-wire were made of 5 μm Pt–10%Rh wire approximately 1 mm in length. For the cold wire, the sensing element was made of 1.27 μm Pt–10%Rh wire, about 1.2 mm in length. The temperature coefficient of the cold wire is 1.69×10^{-3} °C $^{-1}$, determined using a 10 Ω platinum resistance thermometer operated in a Leed and Northrup 8087 bridge with a resolution of 0.010 °C. The hot wires were operated on constant temperature circuits at an overheat ratio of 1.5. The cold wire was operated on a constant current (0.1 mA) circuit with output proportional to θ. The probe was calibrated in the free stream for velocity, yaw angle and temperature using a Pitot-static tube connected to a Furness micromanometer and a thermocouple. A full velocity-yaw angle calibration scheme [19] was used, with a ±20° yaw angle and a 3.0–11.0 m/s velocity range.

Velocity and temperature signals from the anemometer were passed through buck and gain circuits, low-pass filtered and digitised on a personal computer using a 12 bit A/D converter at a sampling frequency of $2f_c = 3500$ Hz, where f_c is the cut-off frequency determined by checking a spectral analyser. The sampling duration was 30 s. The velocity contamination of the cold wire signal was ignored because of the low operating current (0.1 mA). No correction was applied to the instantaneous velocity signals because of a small temperature excess, below 0.8 °C, at the measurement locations.

3. Vortex-shedding frequencies

Fig. 2 presents the u-, v- and θ-spectra, E_u, E_v and E_θ, at $L^* = 2.5$. The spectra in the absence of oscillation display a pronounced peak at $f_s^* = 0.149$, indicating the dominant vortex frequency. The u-spectrum (Fig. 2a) shows a peak at the second harmonic of f_s^*, i.e., $f^* = 0.298$. With the upstream cylinder oscillating, a peak at $f_e^* = 0.025$ appears in the u and v-spectrum, as

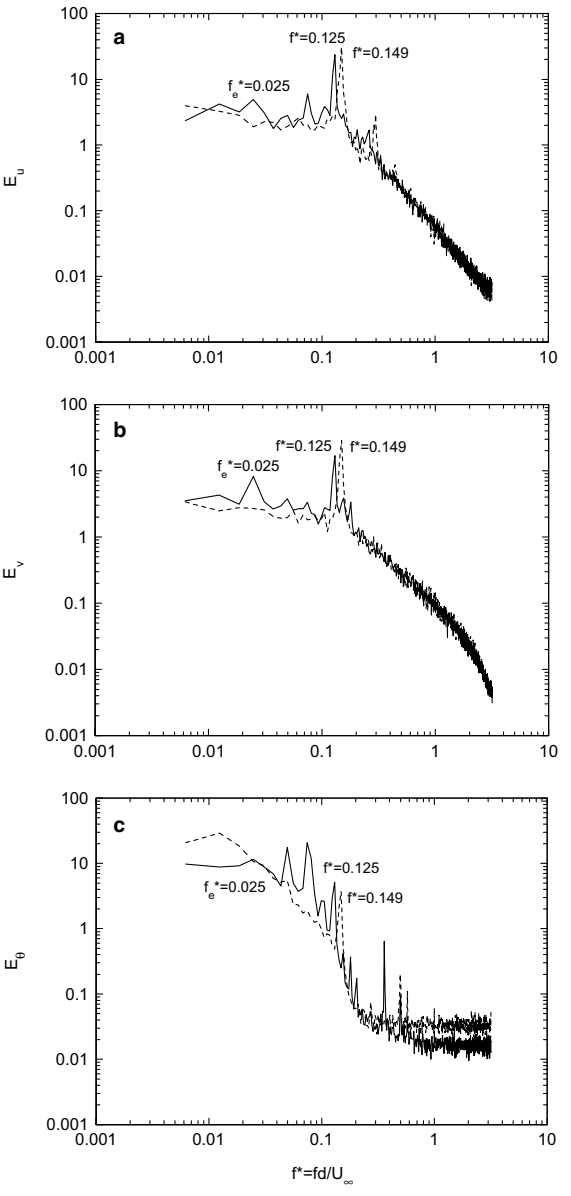

Fig. 2. Spectra of u, v and θ measured between the gap of the cylinders ($x^* = 10$, and $y^* = 1.5$) at $L^* = 2.5$: (a) u; (b) v; (c) θ. Solid line: oscillating upstream cylinder; dashed line: stationary upstream cylinder.

expected. Furthermore, a number of peaks at the harmonics of f_e^* ,up to $5f_e^*$, are discernible in both the u- and v-spectra, among which the one at $f^* = 0.125 = 5f_e^*$ is most pronounced, probably resulting from vortex shedding locked on with the fifth harmonic of f_e^*. The phenomenon that the natural f_s is modified or locked on with the cylinder oscillating frequency has been widely reported in the literature. The extent to which f_s can be modified depends on the oscillation amplitude [20]; larger amplitude corresponds to a greater maximum modification of f_s. In the present context, the different harmonics of the oscillation may compete with each other to lock on f_s. The first harmonic is supposed to have the largest oscillation amplitude. However, this harmonic could not lock on f_s because of a large deviation between them. Apparently, the harmonic that has a minimum deviation from and also lower than the natural f_s (the harmonic that is higher than f_s should have smaller oscillation amplitude) has the greatest potential to lock on f_s. As a result, f_s is locked on with $5f_e$. It is noted that, with a change in f_e^*, the modified vortex-shedding frequency may vary but is always smaller than f_s^*. The result suggests an effective method to modify vortex shedding from a cylinder by oscillating an upstream cylinder and adjusting its oscillating frequency, whose harmonic may dictate the vortex-shedding frequency behind the downstream cylinder.

The θ-spectrum, E_θ (Fig. 2c), displays a pronounced peak at $f_s^* = 0.149$ in the absence of oscillation and a number of peaks at the harmonics of f_e^* once the oscillation is introduced. The peak at the fifth harmonic $f^* = 0.125$ is apparently connected to the dominant vortices, while others are probably linked to the oscillating shear layers separated from the upstream heated cylinder. This can be verified by examining the spectra of hot-wire signals measured between the cylinders.

In order to understand the relationship between the vortical structures generated by the two cylinders, an X-wire was placed at $x^* = -1.25$ and $y^* = 1.5$ to detect possible vortex shedding from the upstream cylinder. Because of large flow fluctuations between the cylinders, the u and v components derived from the X-wire were not so accurate as at $x/d = 10$. This is however not critical since the signals are used only to determine the dominant frequencies. The u- and v- spectra, E_u and E_v (Fig. 3), display a sharp peak at $f^* \approx 0.149$ and a broad peak over $f^* \approx 0.4$–2 for the stationary upstream cylinder. The former peak occurs at the same frequency as the dominant vortices measured behind the downstream cylinder and the latter is ascribed to the instability of shear layers associated with the upstream cylinder. It has been established that the vortex street is not formed in the gap of two cylinders at $L^* = 2.5$ [2]. In fact, the co-existence of the two peaks indicates an incomplete formation of vortices generated by the upstream cylinder [1,17]. Once the cylinder is oscillated, E_u and E_v exhibit one pronounced peak at f_e^* and a few minor ones at the harmonics of f_e^*, up to $6f_e^*$, some of which coincide with those observed in E_θ. Note that the broad peak over $f^* \approx 0.4$–2 now disappears and, meanwhile, the peak at $f^* \approx 0.149$ appears significantly more pronounced, suggesting a complete formation of vortices between the cylinders and enhancement of vortex shedding by the oscillation. This is supported by the laser-induced fluorescence (LIF) flow visualization (Fig. 4) conducted at $Re = 5920$ for $L^* = 2.5$. Two pin holes of 0.5 mm diameter were drilled at ±45° from the leading stagnation point at the mid span of the two cylinders. Smoke, generated from Paraffin oil, of a particle size of about 1 μm in diameter was released from the pin hole, thus providing seeding for flow. A Dantec standard PIV2100 system was used to capture the flow images. More details of the LIF measurements were given in [21]. Vortices are evident between the gap of vortices with the upstream cylinder oscillating (Fig. 4b) but are not observed without (Fig. 4a). It is evident that the upstream cylinder oscillation leads to a change in the flow regime at $L^* = 2.5$ from one-cylinder shedding to "co-shedding" from both cylinders.

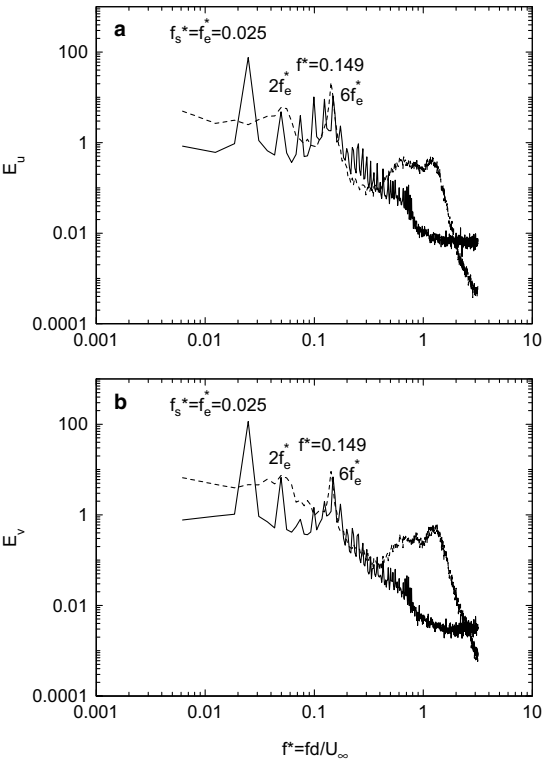

Fig. 3. Spectra of u and v and measured between the gap of the cylinders ($x^* = -1.25$, $y^* = 1.5$) at $L^* = 2.5$: (a) u; (b) v. Solid line: oscillating upstream cylinder; dashed line: stationary upstream cylinder.

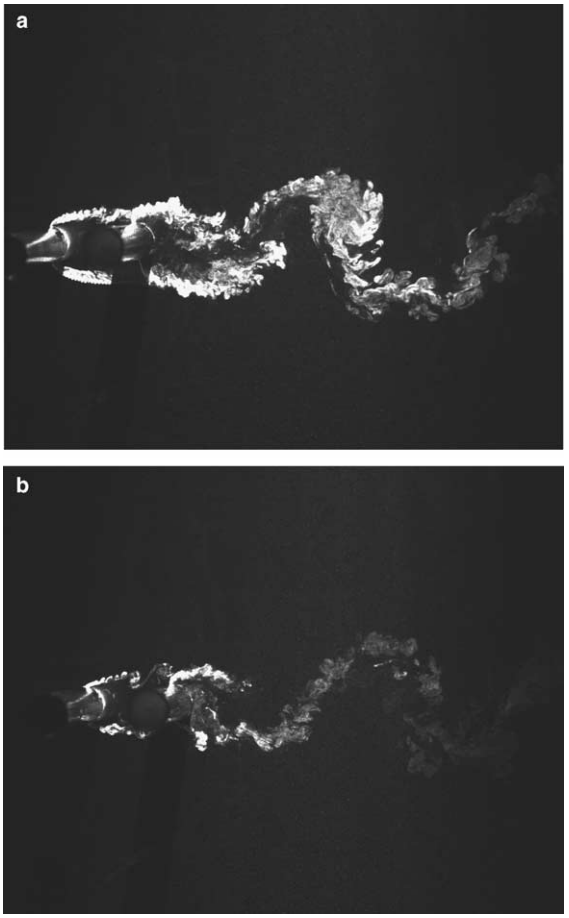

Fig. 4. Photographs of flow visualization at $L/d = 2.5$ and $Re = 5920$: (a) without cylinder oscillation; (b) with cylinder oscillation ($f_e/f_s = 0.17$, $A/d = 0.79$).

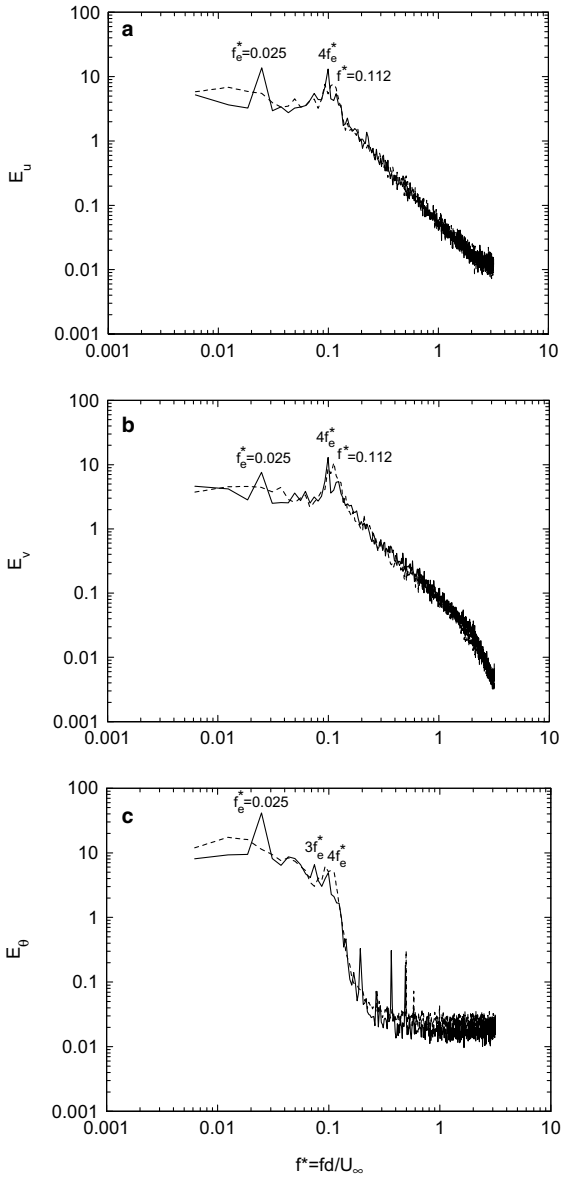

Fig. 5. Spectra of u, v and θ measured behind the cylinders ($x^* = 10$ and $y^* = 1.5$) at $L^* = 4$: (a) u; (b) v; (c) θ. Solid line: oscillating upstream cylinder; dashed line: stationary upstream cylinder.

At $L^* = 4$, E_u, E_v and E_θ at $x^* = 10$ (Fig. 5) all show one pronounced peak at $f_s^* = 0.112$ in the absence of oscillation, apparently resulting from the dominant vortices in the flow. Once the upstream cylinder is oscillated, one strong peak occurs at $f_e^* = 0.025$ and meanwhile the vortex-shedding frequency is reduced to 0.1, locked on with the fourth harmonic of f_e^*. As in the case of $L^* = 2.5$, minor peaks at the other harmonics of f_e^* are also discernible in the spectra.

E_u and E_v (Fig. 6) measured between the stationary cylinders appear qualitatively the same as their counterparts behind the downstream cylinder, exhibiting one pronounced peak at $f_s^* = 0.118$. The observation conforms to previous reports that the frequencies of vortex shedding from the two cylinders are identical [17,22]. In the presence of the upstream cylinder oscillation, however, both E_u and E_v display their most pronounced peak at $5f_e^*$, implying that vortex shedding from the oscillating cylinder is locked on with the fifth harmonic of f_e^*, deviating from vortex shedding from the downstream cylinder, which is locked on with $4f_e^*$ (Fig. 5). The deviation is not well understood at this stage.

It is noteworthy that the vortex-shedding frequency behind the downstream cylinder drops as a result of the upstream cylinder oscillation, irrespective of the L^* value, changing from 0.149 to 0.125 at $L^* = 2.5$ and from 0.112 to 0.1 at $L^* = 4$.

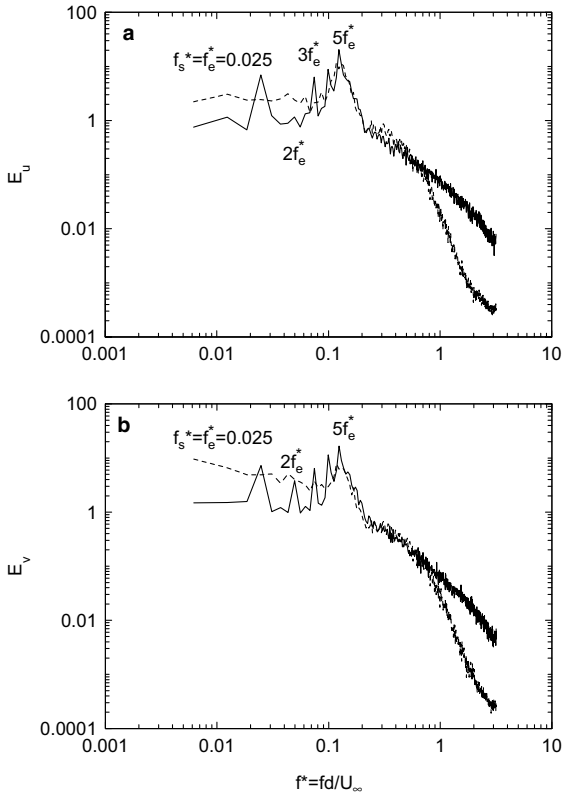

Fig. 6. Spectra of u and v measured between the gap of the cylinders ($x^* = -1.25$, $y^* = 1.5$) at $L^* = 4$: (a) u; (b) v. Solid line: oscillating upstream cylinder; dashed line: stationary upstream cylinder.

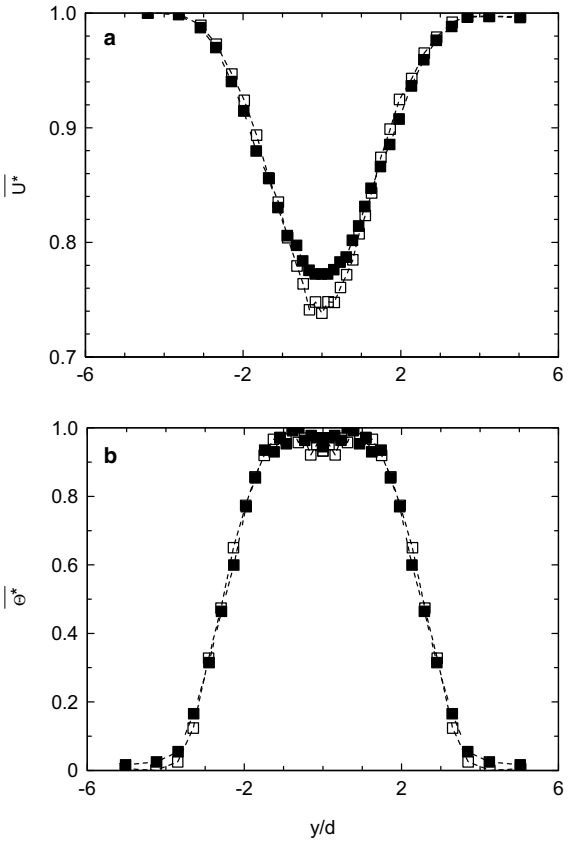

Fig. 7. Cross-flow distributions of (a) mean velocity $\overline{U^*}$ and (b) temperature $\overline{\Theta^*}$ at $L^* = 2.5$ and $x^* = 10$. Open symbol: stationary upstream cylinder; solid symbol: oscillating upstream cylinder.

4. Time-averaged velocity and temperature and Reynolds stresses

Fig. 7 compares the lateral distributions of the mean velocity $\overline{U^*}$ and temperature $\overline{\Theta^*}$ at $L^* = 2.5$ ($x^* = 10$) with and without the upstream cylinder oscillating. The experimental uncertainties in $\overline{U^*}$ and $\overline{\Theta^*}$ are estimated to be 2% and 8%, respectively. The latter is largely caused by the temperature drift in the cold-wire measurement. Both $\overline{U^*}$ and $\overline{\Theta^*}$ are reasonably symmetrical about the flow centreline. The cylinder oscillation causes an appreciable reduction in the maximum velocity defect but appears to have a negligible effect on $\overline{\Theta^*}$. Figs. 8 and 9 present the cross-flow distributions of the Reynolds stresses ($\overline{u^{*2}}, \overline{v^{*2}}, \overline{u^*v^*}$), temperature variance ($\overline{\theta^{*2}}$), and heat fluxes ($\overline{u^*\theta^*}$ and $\overline{v^*\theta^*}$). The experimental uncertainties for $\overline{u^{*2}}, \overline{v^{*2}}, \overline{u^*v^*}, \overline{\theta^{*2}}, \overline{u^*\theta^*}$ and $\overline{v^*\theta^*}$ are estimated to be about 5%, 5%, 5%, 10%, 8% and 8%, respectively. The distributions of $\overline{u^{*2}}, \overline{v^{*2}}$ and $\overline{\theta^{*2}}$ are symmetrical about the flow centerline. So is $\overline{u^*\theta^*}$. On the other hand, $\overline{u^*v^*}$ and $\overline{v^*\theta^*}$ are anti-symmetrical. As a result of oscillation, the $\overline{u^{*2}}$ distribution grows wider, and the maximum $\overline{v^{*2}}, \overline{\theta^{*2}}, \overline{u^*v^*}$ and $\overline{v^*\theta^*}$ all increase appreciably.

The observations are linked to the earlier finding that the upstream cylinder oscillation changes the flow from the reattachment regime to the co-shedding regime (Section 3). This change in the initial condition from the shear layer reattachment to the vortex impingement on the downstream cylinder enhances the cross-flow fluctuation, which is supported by the increased $\overline{v^{*2}}$ (Fig. 8b). As a consequence, more high-speed fluid is entrained into the wake and more slow fluid is transferred towards the free stream. The increased mixing causes a growing width in $\overline{u^{*2}}$ (Fig. 8a) and increased $\overline{\theta^{*2}}$ near the centerline (Fig. 8c), and also an enhancement of the momentum and heat transport (Fig. 9a and c). Note that the cross-flow distribution of $\overline{u^*\theta^*}$ (Fig. 9b) in the presence of oscillation is totally different from that in the absence of oscillation. This is not unexpected in view of two different flow regimes associated with the two cases.

It is worthwhile pointing out that the $\overline{u^{*2}}$ distribution exhibits single peak, regardless of oscillation, whereas its

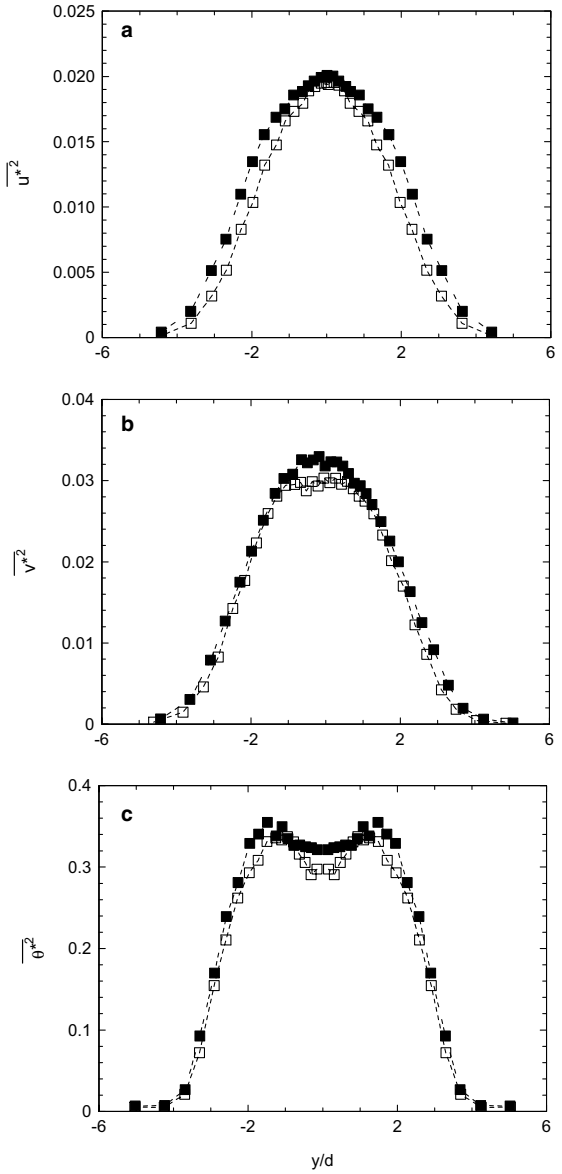

Fig. 8. Cross-flow distributions of velocity and temperature variances at $L^* = 2.5$ and $x^* = 10$: (a) $\overline{u^{*2}}$; (b) $\overline{v^{*2}}$; (c) $\overline{\theta^{*2}}$. Open symbol: stationary upstream cylinder; solid symbol: oscillating upstream cylinder.

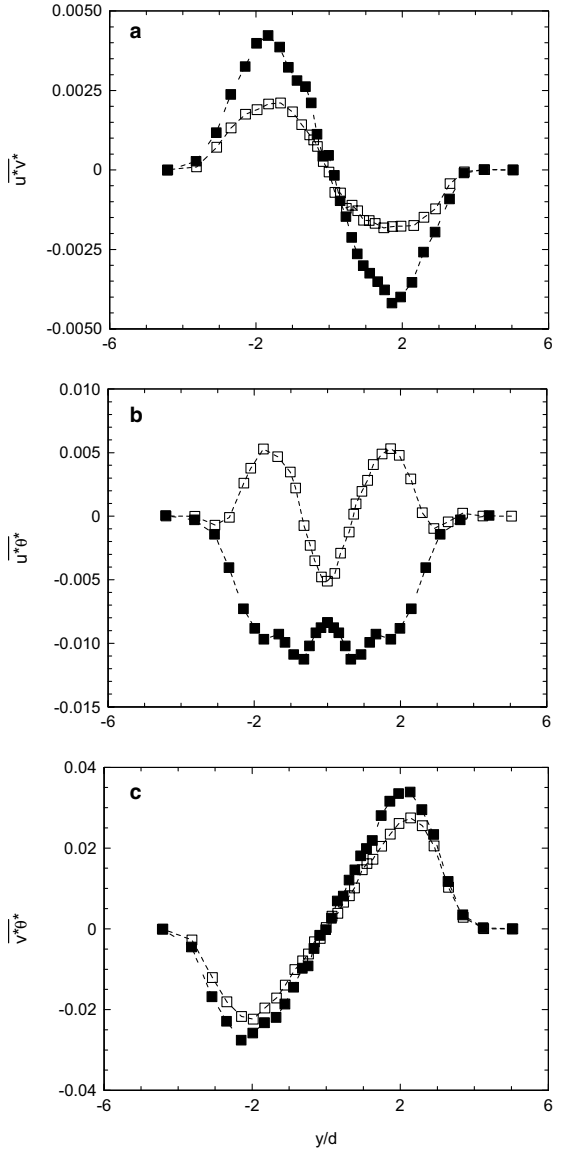

Fig. 9. Cross-flow distributions of Reynolds shear stress and heat fluxes at $L^* = 2.5$ and $x^* = 10$: (a) $\overline{u^*v^*}$; (b) $\overline{u^*\theta^*}$; (c) $\overline{v^*\theta^*}$. Open symbol: stationary upstream cylinder; solid symbol: oscillating upstream cylinder.

counterpart behind an isolated cylinder shows a twin-peak distribution at the same x^* [23]. Two causes may be responsible for the observed difference, that is, vortices are presently weak or lateral spacing between cross-stream vortices is small, compared with a single cylinder case. The wake half-width based on the $\overline{U^*}$ distribution is $1.45d$ and $1.73d$ for the two cases of the non-oscillation and oscillation, respectively, significantly larger than $0.81d$ for a single cylinder wake at $Re = 5830$ [8]. Furthermore, the peaks in $\overline{u^*v^*}$ and $\overline{v^*\theta^*}$ occur at $y/d \approx \pm 2$, while their counterparts behind a single cylinder occur at $y/d \approx \pm 1$ [8]. The observations point to unequivocally increased lateral spacing between cross-stream vortices in the wake of two tandem cylinders.It may be therefore inferred that the vortices are presently rather weak in strength, contributing to the single peak $\overline{u^{*2}}$ distribution.

Figs. 10–12 present the cross-flow distributions of $\overline{U^*}, \overline{\Theta^*}, \overline{u^{*2}}, \overline{v^{*2}}, \overline{\theta^{*2}}, \overline{u^*v^*}, \overline{u^*\theta^*}$ and $\overline{v^*\theta^*}$ at $L^* = 4$, respectively. A number of points are noteworthy. Firstly, $\overline{U^*}, \overline{\Theta^*}, \overline{\theta^{*2}}, \overline{u^*v^*}$ and $\overline{v^*\theta^*}$ are qualitatively similar to

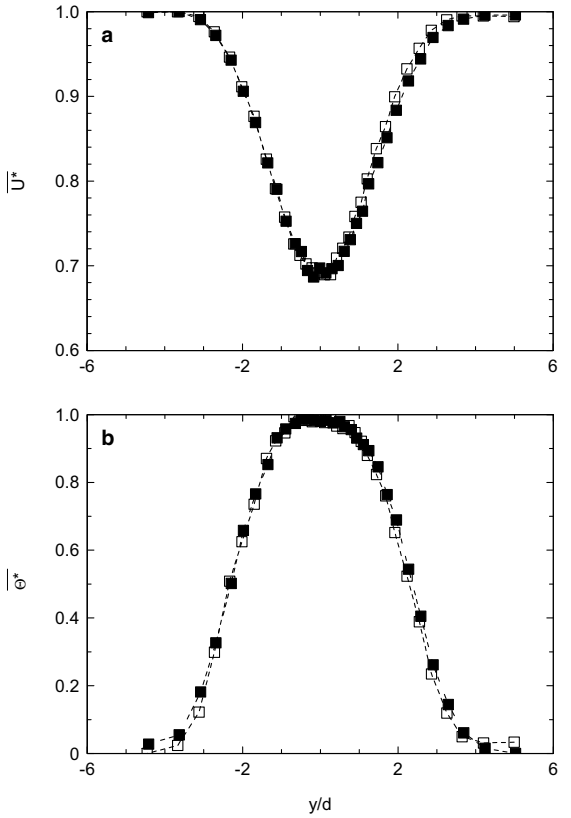

Fig. 10. Cross-flow distributions of mean velocity $\overline{U^*}$ (a) and temperature $\overline{\Theta^*}$ (b) at $L^* = 4$ and $x^* = 10$. Open symbol: stationary upstream cylinder; solid symbol: oscillating upstream cylinder.

those at $L^* = 2.5$. However, unlike their counterparts at $L^* = 2.5$, $\overline{u^{*2}}$ and $\overline{v^{*2}}$ tend to show a twin-peak distribution, which is probably due to increased lateral spacing between cross-stream vortices. Indeed, the mean velocity half-width increases slightly from $1.45d$ at $L^* = 2.5$ to $1.52d$ at $L^* = 4$. Furthermore, compared with the case of $L^* = 2.5$, the maximum velocity defect is appreciably larger, but $\overline{v^{*2}}$ and $\overline{\theta^{*2}}$ are smaller. The difference is again connected to the distinct initial conditions. Secondly, the upstream cylinder oscillation produces an effect very different from that at $L^* = 2.5$. $\overline{U^*}$ is essentially unchanged in the presence of the oscillation. But there is an appreciable decrease in the magnitude of $\overline{v^{*2}}, \overline{u^*v^*}, \overline{u^*\theta^*}$ and $\overline{v^*\theta^*}$, in marked contrast with the case at $L^* = 2.5$, where the quantities all arise in magnitude. The difference in the quantities at $L^* = 2.5$ is largely attributed to the change in the flow regime from the reattachment to the co-shedding once the upstream cylinder is forced to oscillate. At $L^* = 4$, however, the flow regime remains the same with or without the upstream cylinder oscillating; therefore, the oscillation effect on the wake is expected to be different from the case at $L^* = 2.5$. As

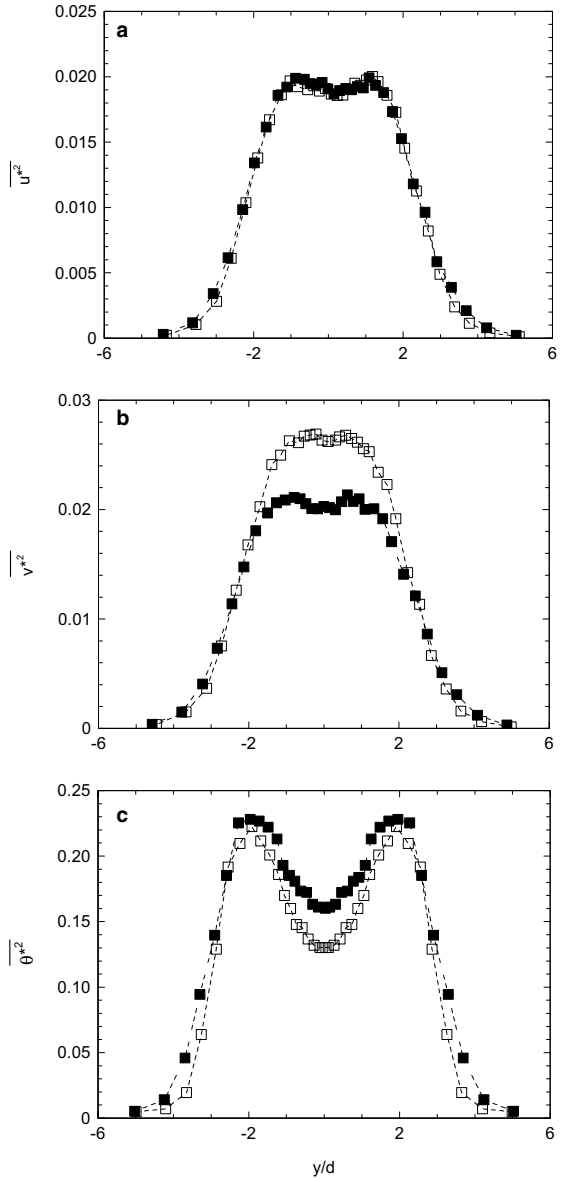

Fig. 11. Cross-flow distributions of velocity and temperature variance at $L^* = 4.0$ and $x^* = 10$: (a) $\overline{u^{*2}}$; (b) $\overline{v^{*2}}$; (c) $\overline{\theta^{*2}}$. Open symbol: stationary upstream cylinder; solid symbol: oscillating upstream cylinder.

noted in E_u and E_v (Figs. 5 and 6), the predominant vortex frequency is $4f_e$ between the cylinders but jumps to $5f_e$ behind the downstream cylinder. Presumably, the interaction between the two types of vortices of different frequencies may accelerate the decay of the vortices behind the downstream cylinder. As a result, $\overline{v^{*2}}$ is considerably reduced and subsequently both momentum ($\overline{u^*v^*}$) and heat transport ($\overline{v^*\theta^*}$) impair. It is noted that the distribution of $\overline{u^*\theta^*}$ is qualitatively unchanged by the

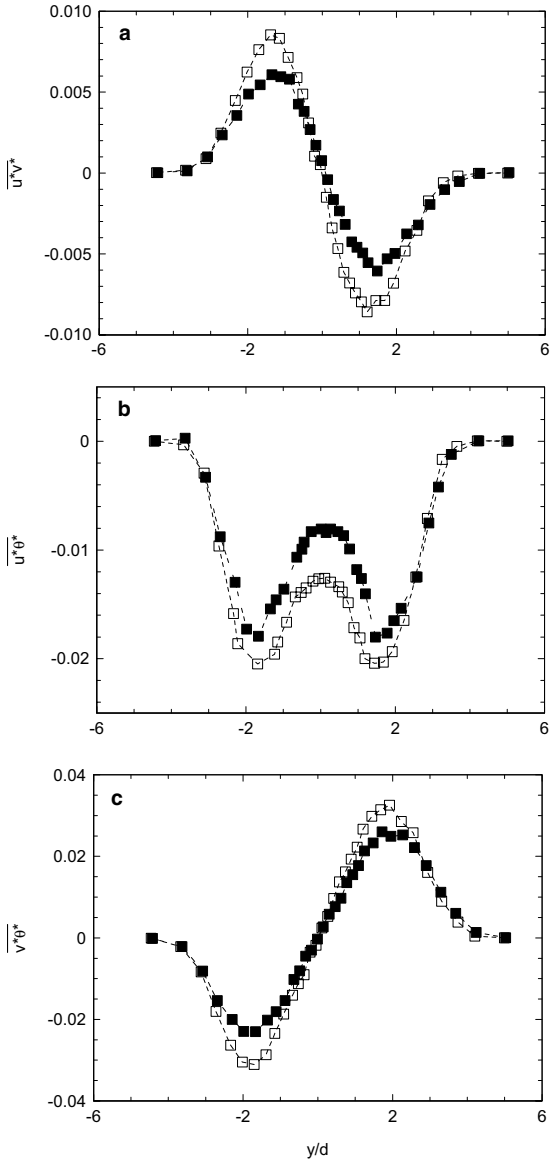

Fig. 12. Cross-flow distributions of Reynolds shear stress and heat fluxes at $L^* = 4.0$ and $x^* = 10$: (a) $\overline{u^*v^*}$; (b) $\overline{u^*\theta^*}$; (c) $\overline{v^*\theta^*}$. Open symbol: stationary upstream cylinder; solid symbol: oscillating upstream cylinder.

oscillation. This is reasonable since the flow regime is unaffected at $L^* = 4$ by the oscillation.

5. Turbulent Prandtl number

The turbulent Prandtl number, Pr_t, defined by [24]

$$Pr_t = \frac{\overline{uv}/(\partial\overline{U}/\partial y)}{\overline{v\theta}/(\partial\overline{\Theta}/\partial y)} \quad (1)$$

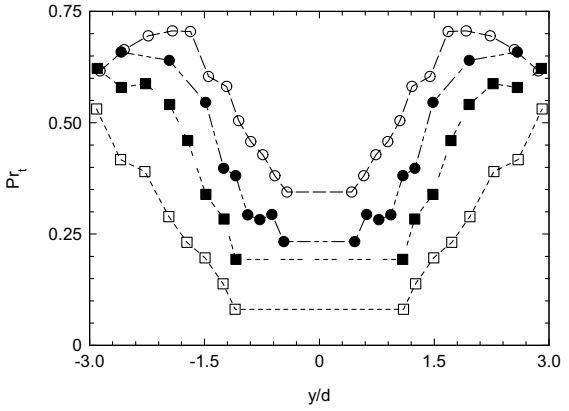

Fig. 13. Cross-flow distributions of turbulent Prandtl number Pr_t at $x^* = 10$. Circle: $L^* = 4$; square: 2.5. Open symbol: stationary upstream cylinder; solid symbol: oscillating upstream cylinder.

is given in Fig. 13. The mean velocity and temperature gradients, $\partial\overline{U}/\partial y$ and $\partial\overline{\Theta}/\partial y$, were obtained from a least-square sixth-order polynomial fit to $\overline{U}$ and $\overline{\Theta}$. This method of determining Pr_t is similar to that used by [25]. The resulting uncertainty in Pr_t was estimated from the uncertainties in $\overline{uv}, \overline{v\theta}$ and $\partial\overline{\Theta}/\partial\overline{U}$ and was found to be about 17%. Pr_t is not shown near $y^* = 0$, where a singular point occurs. Pr_t is in the order of 1 and declines towards $y^* = 0$, suggesting that heat transport is progressively more effective than momentum transport towards the wake centreline.

Without the oscillation, Pr_t is significantly larger at $L^* = 4$ than at $L^* = 2.5$, which correspond to the co-shedding regime and the reattachment regime, respectively. Examining $\overline{U^*}, \overline{\Theta^*}, \overline{u^*v^*}$ and $\overline{v^*\theta^*}$ (Figs. 7, 9, 10 and 12) unveils that, while the difference in $\partial\overline{U^*}/\partial y, \partial\overline{\Theta^*}/\partial y$ and $\overline{v^*\theta^*}$ is relatively small between the two regimes, $\overline{u^*v^*}$ in the reattachment regime is only about one fourth that in the co-shedding regime. The observation suggests a substantially more effective momentum transport in the co-shedding regime than in the reattachment regime, which accounts for the higher Pr_t at $L^* = 4$.

The oscillation effect is opposite for the two cases; Pr_t drops at $L^* = 4$ but goes up at $L^* = 2.5$. At $L^* = 2.5$, the upstream cylinder oscillation gives rise to a switch from the flow reattachment regime to the co-shedding regime. This regime change is responsible for rising Pr_t. In fact, it can be inferred from Figs. 7 and 9 that the oscillation causes little variation in $\partial\overline{U^*}/\partial y$ or $\partial\overline{\Theta^*}/\partial y$ and an increase in the $\overline{v^*\theta^*}$ magnitude by only 17%. However, $\overline{u^*v^*}$ climbs more than 100% in magnitude because of the regime change, overwhelming other effects. At $L^* = 4$, with the flow regime unchanged, the oscillation has essentially no influence on $\overline{U^*}$ and $\overline{\Theta^*}$ or $\partial\overline{U^*}/\partial y$ and $\partial\overline{\Theta^*}/\partial y$, but reduces $\overline{u^*v^*}$ by about 40% and $\overline{v^*\theta^*}$

by 30%, thus resulting in a decline in Pr_t. It may be concluded that the momentum transport is more liable to the oscillation effect than the heat transport.

6. Conclusions

The turbulent cylinder wake behind a longitudinally oscillating cylinder has been investigated. The investigation is conducted at large oscillating amplitude ($A^* = 0.79$) and a low frequency ratio ($f_e/f_s = 0.17$ for $L^* = 2.5$ and 0.24 for $L^* = 4$), leading to following conclusions:

1. For all L^* investigated, the frequency of vortex shedding from the stationary cylinder is found to be modified by the upstream cylinder oscillation; it is locked on with one harmonic of the oscillating frequency (f_e), which is $5f_e$ at $L^* = 2.5$ and $4f_e$ at $L^* = 4$. This harmonic frequency is nearest to and below that of natural vortex shedding. In the co-shedding flow regime behind two stationary cylinders, the predominant vortex frequency in the gap of the cylinders is identical to that behind the downstream cylinder. However, the upstream cylinder oscillation may cause the two frequencies to slightly deviate from each other, which has yet to be better understood in future investigations.
2. The oscillation effect on the flow depends on L^*. While the flow regime at $L^* = 4$ remains unchanged by the upstream cylinder oscillation, that at $L^* = 2.5$ is altered from the reattachment to the co-shedding regime. As a result, the oscillation gives rise to a decrease in the velocity defect at $L^* = 2.5$ but no change at $L^* = 4$. Furthermore, $\overline{v^{*2}}, \overline{u^*v^*}, \overline{u^*\theta^*}$ and $\overline{v^*\theta^*}$ is weakened in strength at $L^* = 4$, but increased at $L^* = 2.5$.
3. The upstream cylinder oscillation has an appreciable effect on turbulent Prandtl number Pr_t. It is found that the momentum transport is significantly more effective in the co-shedding regime than in the reattachment regime, resulting in a larger Pr_t at $L^* = 4$ than at $L^* = 2.5$. Therefore, with the upstream cylinder oscillating, the flow regime change from reattachment to co-shedding at $L^* = 2.5$ is associated with a rise in Pr_t. On the other hand, at $L^* = 4$ the oscillation does not change the flow regime and adversely affects momentum transport more than heat transport, contributing to a smaller Pr_t.

Acknowledgements

Authors wish to acknowledge support given to them by the Central Research Grant of The Hong Kong Polytechnic University through Grant G-YW74.

References

[1] T. Igarashi, Characteristics of the flow around two cylinders arranged in tandem, 1st Report, Bull. JSME B24 (1981) 323–331.
[2] M.M. Zdravkovich, The effects of interference between circular cylinders in cross flow, J. Fluids Struct. 1 (1987) 239–261.
[3] P.M. Moretti, Flow-induced vibrations in arrays of cylinders, Annu. Rev. Fluid Mech. 25 (1993) 99–114.
[4] V. Kolář, D.A. Lyn, W. Rodi, Ensemble-averaged measurements in the turbulent near wake of two side-by-side square cylinders, J. Fluid Mech. 346 (1997) 201–237.
[5] D. Sumner, S.J. Price, M.P. Paidoussis, Flow-pattern identification for two staggered circular cylinders in cross-flow, J. Fluid Mech. 411 (2000) 263–303.
[6] J.-C. Lin, Y. Yang, D. Rockwell, Flow past two cylinders in tandem: instantaneous and averaged flow structure, J. Fluids Struct. 16 (2002) 1059–1071.
[7] Y. Zhou, H.J. Zhang, M.W. Yiu, The turbulent wake of two side-by-side circular cylinders, J. Fluid Mech. 458 (2002) 303–332.
[8] M. Matsumura, R.A. Antonia, Momentum and heat transport in the turbulent intermediate wake of a circular cylinder, J. Fluid Mech. 250 (1993) 651–668.
[9] M.W. Yiu, Y. Zhou, Y. Zhu, Passive scalar transport in a turbulent cylinder wake in the presence of a downstream cylinder, Flow Turbulence Combust. 72 (2004) 449–461.
[10] W.K. George, The self-preservation of turbulent flows and its relation to initial conditions and coherent structures, in: W.K. George, R.E.A. Arndt (Eds.), Advances in Turbulence, Hemisphere, New York, 1989, pp. 39–73.
[11] P.B.V. Johansson, W.K. George, M.J. Gourlay, Equilibrium similarity, effects of initial conditions and local Reynolds number on the axisymmetric wake, Phys. Fluids 15 (2003) 603–617.
[12] Y. Zhou, R.A. Antonia, Memory effects in a turbulent plane wake, Expts. Fluids 19 (1995) 112–120.
[13] C. Gau, S.X. Wu, H.S. Su, Synchronization of vortex shedding and heat transfer enhancement over a heated cylinder oscillating with small amplitude in streamwise direction, J. Heat Transfer 123 (2001) 1139–1148.
[14] W.C. Lai, Y. Zhou, R.M.C. So, T. Wang, Interference between a stationary and a vibrating cylinder wake, Phys. Fluids 15 (2003) 1687–1695.
[15] N. Mahir, D. Rockwell, Vortex formation from a forced system of two cylinders. Part I: Tandem arrangement, J. Fluid Struct. 10 (1996) 473–489.
[16] N. Mahir, D. Rockwell, Vortex formation from a forced system of two cylinders. Part II: Side-by-side arrangement, J. Fluid Struct. 10 (1996) 491–500.
[17] G. Xu, Y. Zhou, Strouhal numbers in the wake of two inline cylinders, Expts. Fluids 37 (2004) 248–256.
[18] P.K. Stansby, The effects of end plates on the base pressure coefficient of a circular cylinder, Aeronaut. J. 78 (1974) 36–37.
[19] L.W.B. Browne, R.A. Antonia, L.P. Chua, Calibration of X-probe for turbulent flow measurements, Expts. Fluids 7 (1989) 201–208.

[20] A. Ongoren, D. Rockwell, Flow structure from an oscillating cylinder. Part II. Mode competition in the near wake, J. Fluid Mech. 191 (1988) 225–245.
[21] L. Cheng, Y. Zhou, M.M. Zhang, A perturbation on interactions between vortex shedding and free vibration, J. Fluids Struct. 17 (2003) 887–901.
[22] S. Ishigai, E. Nishikawa, K. Nishimura, K. Cho, Experimental study on structure of gas flow in tube banks with tube axes normal to flow (Part 1, Karman vortex flow around two tubes at various spacings), Bull. Jpn. Soc. Mech. Eng. 5 (86) (1972) 949–956.
[23] Y. Zhou, R.A. Antonia, A study of turbulent vortices in the wake of a cylinder, J. Fluid Mech. 253 (1993) 643–661.
[24] R.A. Antonia, Y. Zhou, M. Matsumara, Spectral characteristics of momentum and heat transfer in the turbulent wake of a circular cylinder, Exp. Thermal Fluid Sci. 6 (1993) 371–375.
[25] Y. Zhou, R.M.C. So, M.H. Liu, H.J. Zhang, Complex turbulent wakes generated by two and three side-by-side cylinders, Int. J. Heat Fluid Flow 12 (2000) 125–133.